 CMC, vol.28, no.2, pp.165-179, 2012

Chemical Stresses Induced by Boundary Layer Diffusion in a Cylindrical Sandwich Composite

Sun-Chien Ko[1,2], Chen-Ti Hu[1], Sanboh Lee[1], Y.T. Chou[3]

Abstract: The chemical stresses developed in a cylindrical sandwich composite during radial boundary layer diffusion have been investigated. The system consists of a thin layer A of circular cross section sandwiched between two semi-infinite outer layers B, with the diffusivity of diffusant in A (D_A) being much greater than that in B (D_B). Two boundary conditions, the constant surface concentration and the instantaneous surface concentration, were considered. The concentration distributions were obtained by the Bessel-Laplace transform method. The stress functions were solved analytically based on the linear elasticity. Numerical computations were performed to illustrate the effects of the diffusivity ratio (D_A/D_B) and of the thickness of the central layer A on stress distributions. The results show that the induced stress in layer A increases as the diffusivity ratio, or its thickness, increases, in consistency with the general findings for composites of rectangular geometry.

Keywords: Chemical stress; Boundary layer diffusion; Cylindrical sandwich composite

1 Introduction

Chemical stresses can be developed in an elastic medium during diffusion [Prussin (1961); Li (1978)]. These induced stresses may affect many material properties for their applications. For example, they may improve the mechanical property of steels [Read-Hill and Abbaschian (1994)], but on the other hand degrade the electrical property of semiconductor devices [Schwuttke and Queisser (1962); Miller, Moore and Morre (1962)]. Recently, Christensen and Newman (2006) reported that the premature structural failure of the electrode of Li-ion batteries was caused

[1] Department of Materials Science and Engineering, National Tsing Hua University, Hsinchu, Taiwan

[2] Advanced Technology Research Laboratory, Telecommunication Laboratories, Chunghwa Telecom Company, Taoyuan, Taiwan

[3] Department of Chemical Engineering and Materials Science, University of California, Irvine, California 92697, U.S.A

by the chemical stress. The interest in research on this subject was renewed. Yang (2010) considered that, in addition to solid diffusion, the solid reaction would significantly enhance the stress on the plate surface. Deshpande, Cheng, Verbrugge and Timmons (2011) investigated the diffusion-induced stresses in phase transforming electrode using a core-shell structural model. The same authors [Deshpande, Cheng and Verbrugge (2010)] also modeled the diffusion-induced stress in nanowire electrode structure where the surface strain energy was comparable with the bulk strain energy. More recently, Bhandakkar and Gao (2011) proposed the cohesive model of crack nucleation in a cylindrical electrode under axisymmetric diffusion-induced stresses. On the other hand, the analysis of chemical stress has been extended to the grain boundary region during grain boundary diffusion [Wang, Chou and Lee (1998); Wang, Chou and Lee (2001)], and to the layered composite during boundary-layer diffusion [Lin, Ko and Lee (2004); Ko, Lee and Chou (2005)]. It has been pointed out that both grain boundary diffusion and boundary layer diffusion can be analyzed based on the same mathematical model, in which the material system is a layered composite of the BAB type. The central layer A is extremely thin, and has a much greater diffusivity of the diffusant than the two semi-infinite B layers. The only difference between the two models is that in grain boundary diffusion, layer A has the same chemical composition as layer B; in boundary layer diffusion, the two layers have different compositions but no interdiffusion.

In recent years, the layered composites, especially the nano-layered composites, were increasingly used in the semiconductor devices. One of the applications is the vertical cavity surface emitting laser (VCSEL), which is favored as a transmitter for optical data links. The wet oxidization of Al-containing semiconductor produces a mechanically robust and a low refractive index Al-oxide [Dallesasse, Holonyak , Sugg, Richard and El-Zein (1990); Guha, Agahi, Pezeshki, Kash, Kisker and Bojarczuk (1996)]. This oxide layer provides the current and optical apertures in the VCSEL fabrication [Huffaker, Deppe, Kumar and Rogers (1994); Hayashi, Mukaihara, Hatori, OhnoKi, Matsutani, Koyama and Iga (1995)], resulting in a remarkable low threshold current and a high efficient performance [Larson, Coldren, Spruytte, Petersen and Harris (2000); Deppe, Huffaker, Oh, Deng and Deng (1997)]. The oxide layer confines the current to inject into the quantum wells accurately, and its low refractive index induces index-guide optical confinement for single mode evolution [Weigl, Grabherr, Michalzik, Reiner and Ebeling (1996); Nishiyama, Arai, Shinada, Suzuki, Koyama and Iga (2000)]. However, the porosity was observed occasionally due to the high stress developed during the application of wet oxidation to VCSEL [Christensen and Newman (2006)]. In the design of the VCSEL and other nano semiconductor device, the cylindrical composites are used as often

as the rectangular units [Choquette, Geib, Ashby, Twesten, Blum, Hou, Follstaedt, Hammons, Mathes and Hull (1997)]. Recently the boundary layer diffusion in a cylindrical composite with the surface concentration source was analyzed [Ko, Lee and Chou (2009)]. This prompted us to investigate the chemical stresses for the same geometrical system. The details of the concentration distribution and stress analysis are given in the next two sections.

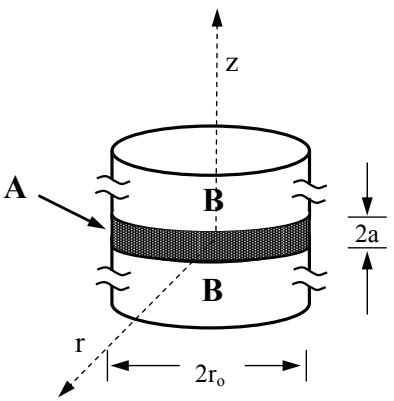

Figure 1: Schematic diagram showing a thin circular layer A sandwiched between two outer layers B in a cylindrical coordinate system.

2 Concentration distribution

Consider a cylindrical sandwich composite of circular cross section with a thin central layer A of radius r_0 and thickness $2a$, sandwiched between two semi-infinite outer layers B, as shown in Fig.1. Layer A and layer B have different chemical compositions, but no significant interdiffusion. In the cylindrical coordinate system, layer A and layer B are located in the regions $r \le r_0, |z| \le a$ and $r \le r_0, a \le |z|$, respectively, with the origin at the center of layer A. The diffusant, which has a chemical composition different from those of A and B, is placed on the lateral surface at $r = r_o$. The diffusivity of the diffusant is much greater in layer A than in layer B, ($D_A >> D_B$). Both layers are assumed to be isotropic materials. The diffusant follows the Fickian law in each layer as:

$$D_A \left(\frac{\partial^2 C_A}{\partial r^2} + \frac{1}{r}\frac{\partial C_A}{\partial r} + \frac{\partial^2 C_A}{\partial z^2} \right) = \frac{\partial C_A}{\partial t} \quad |z| \le a \tag{1a}$$

in layer A, and

$$D_B\left(\frac{\partial^2 C_B}{\partial r^2}+\frac{1}{r}\frac{\partial C_B}{\partial r}+\frac{\partial^2 C_B}{\partial z^2}\right)=\frac{\partial C_B}{\partial t} \quad a\le|z| \tag{1b}$$

in layer B, where D_A and D_B are diffusion constants of the diffusant in layers A and B, respectively. D_A is also assumed to be much greater than D_B. The concentration and flux at interfaces $z=\pm a$ satisfy the continuity, i.e. ,

$$C_A(r,z=\pm a,t)=C_B(r,z=\pm a,t) \tag{2a}$$

and

$$D_A\frac{\partial C_A(r,z=\pm a,t)}{\partial z}=D_B\frac{\partial C_B(r,z=\pm a,t)}{\partial z} \tag{2b}$$

According to Whipple (1954), the boundary equations Eq. (2) can be modified.

Because of geometric symmetry, C_A is an even function of z. If $r>>a$, C_A can be approximated as

$$C_A(r,z,t)=C_{A0}(r,t)+\frac{z^2}{2}C_{A2}(r,t) \tag{3a}$$

Then Eq. (1a) gives the zeroth order of z as (neglecting the terms of order z^2),

$$D_A\left(\frac{\partial^2 C_{A0}}{\partial r^2}+\frac{1}{r}\frac{\partial C_{A0}}{\partial r}+C_{A2}\right)=\frac{\partial C_{A0}}{\partial t} \tag{3b}$$

Neglecting the terms of order a^2, the boundary conditions Eqs. (2a) and (2b) at $z=\pm a$ are

$$C_{A0}=C_B \tag{4a}$$

$$D_B\frac{\partial C_B}{\partial z}=\pm D_A a C_{A2} \tag{4b}$$

Eliminating C_{A0} and C_{A2}, we obtain

$$D_A\left(\frac{\partial^2 C_B}{\partial r^2}+\frac{1}{a}\frac{\partial C_B}{\partial r}\right)\pm\frac{D_B}{a}\frac{\partial C_B}{\partial z}=\frac{\partial C_B}{\partial t} \text{ at } z=\pm a \tag{5a}$$

Equation (5a) is a single homogeneous boundary condition at $z=a$. Using Eq. (1b), an alternative equation of Eq. (5a) is

$$D_A\frac{\partial^2 C_B}{\partial z^2}\mp\frac{D_B}{a}\frac{\partial C_B}{\partial z}=\left(\frac{D_A}{D_B}-1\right)\frac{\partial C_B}{\partial t} \text{ at } z=\pm a \tag{5b}$$

The problem becomes to solve Eq. (1b) with the constraint, Eq. (5b). In practice, the diffusion flow proceeds under two different source conditions, either with a constant or an instantaneous surface source.

2.1 Instantaneous surface concentration source

Assume no diffusant inside the sample. On the outer surface deposites a very thin layer of diffusant of M per unit area at room temperature, and then allow the system to diffuse at an elevated temperature. The initial condition is $C_B(r,z,t=0) = M\delta_D(r=a,z)$ and the boundary condition is $\partial C_B(r=a,z,t)/\partial r = 0$, where δ_D is the Dirac delta function. This problem can be solved using the Bessel-Laplace transform. The concentration after the transform is

$$\Phi_n = \frac{-(\frac{D_A}{D_B}-1)\frac{\mu_n^2}{r_0}J_0(\mu_n)M}{[D_A(\frac{\mu_n}{r_0})^2+\frac{D_B}{a}\sqrt{(\frac{\mu_n}{r_0})^2+\frac{\lambda}{D_B}}+\lambda][(\frac{\mu_n}{r_0})^2+\frac{\lambda}{D_B}]} \times \exp[-\sqrt{(\frac{\mu_n}{r_0})^2+\frac{\lambda}{D_B}}(z-a)] + \frac{r_0 J_0(\mu_n)M}{D_B[\mu_n^2+\frac{\lambda}{D_B}]} \quad (6a)$$

and the inverse transform of Eq. (6a) is

$$\frac{C_B(r,z,t)}{2M/r_0} = 1+\sum_{n=1}^{\infty}\frac{J_0(\mu_n\frac{r}{r_0})}{J_0(\mu_n)}\exp[-(\frac{\mu_n}{\beta})^2] - \sum_{n=1}^{\infty}\frac{J_0(\mu_n\frac{r}{r_0})}{J_0(\mu_n)}(\frac{\mu_n}{\beta})\int_1^{\Delta}\exp[-(\frac{\mu_n}{\beta})^2\sigma]erfc\left[\frac{1}{2}\sqrt{\frac{\sigma-1}{\sigma-\Delta}}(\xi+\frac{\sigma-1}{\delta})\right]d\sigma \quad (6b)$$

where

$$\beta = r_0/\sqrt{D_B t} \quad (7a)$$

$$\Delta = D_A/D_B \quad (7b)$$

$$\delta = a(\Delta-1)/\sqrt{D_B t} \quad (7c)$$

$$\xi = (z-a)/\sqrt{D_B t} \quad (7d)$$

and μ_n is the positive nth root of the first kind of Bessel function of first order, $J_1(r)=0$. J_0 is the first kind of Bessel function of the zeroth order. The zeroth order concentration C_A can be obtained from the concentration C_B at $z=a$. That is

$$\frac{C_A(r,t)}{2M/r_0} = 1+\sum_{n=1}^{\infty}\frac{J_0(\mu_n\frac{r}{r_0})}{J_0(\mu_n)}\exp\left[[\delta(\frac{\mu_n}{\beta})^2]^2-(\frac{\mu_n}{\beta})^2\right]erfc[\delta(\frac{\mu_n}{\beta})^2] \quad (8)$$

The concentration C_A of order z^2 is neglected.

2.2 Constant surface concentration source

The concentration at the outer surface $r = r_0$ is maintained constant C_0 at all times. Initially no diffusant is inside the circular sandwich composite. The boundary surface condition and the initial condition are $C_B(r = r_0, z, t) = C_0$ and $C_B(r, z, t = 0) = 0$, respectively. Again this problem can be solved using Bessel-Laplace transformation. The zeroth order concentration C_A was obtained by Ko, Lee and Chou (2009) as

$$\frac{C_A(r,t)}{C_0} = 1 - 2\sum_{n=1}^{\infty} \frac{J_0(\alpha_n \frac{r}{r_0})}{\alpha_n J_1(\alpha_n)} \exp\left[[\delta(\frac{\alpha_n}{\beta_0})^2]^2 - (\frac{\alpha_n}{\beta})^2\right] erfc[\delta(\frac{\alpha_n}{\beta})^2] \tag{9}$$

where α_n is the positive nth root of first kind of Bessel function of the zeroth order,$J_0(r)$. Note that the concentration in layer A is an approximate solution in which the terms of z^2 are neglected.

It is noted that for a cylindrical sandwich composite, the concentration functions C_A, given by Eq. (8) and Eq. (9), are dependent on the inner dimension of the sample. They are functions of the parameter,δ, which in turn is a function of the half-thickness a of the central layer. Such a feature is unique in boundary layer diffusion, and is different from the boundary effect in mass (or heat) flow in hollow and coaxial composite cylinders [Carslaw and Jaeger (1959); Crank (1975)].

3 Analysis of stress distributions

From the concentration distributions given above we proceed to determine the chemical stresses developed in the system, which for simplicity is assumed to be elastically isotropic. Because the concentration in the outer layer B is negligibly small and the dimension of B is sufficiently large, the stresses in layer B are assumed to be zero. Also, since the thickness of layer A is very small, the stresses in the axial direction in layer A can be set to be zero. Similar to the derivation of thermal stresses [Timoshenko and Goodier (1970)], the stresses developed in layer A during the radial boundary layer diffusion can be determined in terms of concentration functions by the chemical stress-strain (σ- ε) relations in cylindrical coordinates:

$$\sigma_r = \frac{E}{1-\nu^2}\left[\varepsilon_r + \nu\varepsilon_\theta - (1+\nu)\frac{\bar{V}\mathrm{C}}{3}\right] \tag{10a}$$

$$\sigma_\theta = \frac{E}{1-\nu^2}\left[\varepsilon_\theta + \nu\varepsilon_r - (1+\nu)\frac{\bar{V}C}{3}\right] \tag{10b}$$

where C is the concentration. E, ν and $\bar{V}$ are the Young's modulus, Poisson's ratio and the partial molal volume, respectively. Note that $\bar{V}$ is positive if the diffusant

is an interstitial atom, or if it is a substitutional atom with an atomic radius greater than that of the host atom. On the other hand, $\bar{V}$ is negative if the diffusant is a substitutional atom with an atomic radius smaller than that of the host atoms. The shear stress $\sigma_{r\theta}$ is zero because of the symmetry. (The concentration function C is independent ofθ.). The force equilibrium then gives

$$\frac{\partial \sigma_r}{\partial r} + \frac{\sigma_r - \sigma_\theta}{r} = 0 \tag{11}$$

After a further substitution of $\varepsilon_r = \partial u/\partial r$ and $\varepsilon_\theta = u/r$ where u is the radial displacement, Eq. (11) becomes a second order differential equation,

$$\frac{d^2u}{dr^2} + \frac{1}{r}\frac{du}{dr} - \frac{u}{r^2} = (1+\nu)\frac{\bar{V}}{3}\frac{\partial C}{\partial r} \tag{12}$$

For a gaseous diffusion source, Eq. (12) can be solved with boundary conditions $u(r=0)=0$, and $\sigma_r(r=r_0)=0$. The solution is

$$u(r) = (1+\nu)\frac{\bar{V}}{3r}\int_0^r rCdr + \frac{(1-\nu)\bar{V}r}{3r_0^2}\int_0^{r_0} Crdr \tag{13}$$

From the radial displacement, the radial and tangential stresses are found to be

$$\sigma_r = \frac{\bar{V}E}{3}\left(\frac{1}{r_0^2}\int_0^{r_0} Crdr - \frac{1}{r^2}\int_0^r Crdr\right) \tag{14a}$$

$$\sigma_\theta = \frac{\bar{V}E}{3}\left(-C + \frac{1}{r_0^2}\int_0^{r_0} Crdr + \frac{1}{r^2}\int_0^r Crdr\right) \tag{14b}$$

Eqs. (14a) and (14b) indicate that both σ_r and σ_θ are zero at a constant C. This is the case when the diffusion time approaches infinity.

Since there is no shear stress in the cylindrical sandwich composite, σ_r and σ_θ are the principal stresses. Also, under the condition of plane stress, $\sigma_z = 0$, and the principal shear stresses are given by

$$(\sigma_r - \sigma_\theta)/2 = \frac{\bar{V}E}{6}\left(C - \frac{2}{r^2}\int_0^r Crdr\right) \tag{15a}$$

$$(\sigma_\theta - \sigma_z)/2 = \sigma_\theta/2 \tag{15b}$$

$$(\sigma_r - \sigma_z)/2 = \sigma_r/2 \tag{15c}$$

Note that the plastic yielding is determined either by the largest principal shear stress (Tresca criterion) or by the root mean square of these principal shear stresses (von Mises criterion). We now consider two separate cases based on the surface source used:

3.1 Instantaneous surface concentration source

Substituting Eq. (8) into Eqs. (14a) and (14b), we obtain the radial and tangential stresses for the case of instantaneous surface concentration source to be

$$\sigma_r = -\frac{2\overline{V}EM}{3}\sum_{n=1}^{\infty}\frac{J_1(\mu_n\frac{r}{r_0})}{\mu_n r J_0(\mu_n)}\exp\left[[\delta(\frac{\mu_n}{\beta})^2]^2-(\frac{\mu_n}{\beta})^2\right]erfc[\delta(\frac{\mu_n}{\beta})^2] \tag{16a}$$

$$\sigma_\theta = \frac{2\overline{V}EM}{3}\sum_{n=1}^{\infty}\frac{1}{\mu_n J_0(\mu_n)}[\frac{1}{r}J_1(\mu_n\frac{r}{r_0})-(\frac{\mu_n}{r_0})J_0(\mu_n\frac{r}{r_0})]\exp\left[[\delta(\frac{\mu_n}{\beta})^2]^2-(\frac{\mu_n}{\beta})^2\right]$$
$$\text{erfc}[\delta(\frac{\mu_n}{\beta})^2] \tag{16b}$$

Using Eq. (16), we plot in Figs. $2(a)-(c)$ the stress components developed in the cylindrical sandwich composite with the instantaneous surface concentration source. The radial stress at any given radial distance decreases with increasing time (See Fig.2(a).). It can be seen from Fig. $2(b)$ that the tangential stress near the outer surface decreases from a very large value (approaching infinity) to zero with increasing time. The tangential stress at the center is equal to the radial stress due to the equalities, $\lim_{r\to 0}\{J_1(\mu_n r/r_0)/\mu_n r\} = 1/2r_o$ in Eq.(16a) and $\lim_{r\to 0}\{J_1(\mu_n r/r_0)/\mu_n r - J_0(\mu_n r/r_0)/r_0\} = -1/2r_0$ in Eq.(16b). It is noted that the tangential stress is infinite at the outer surface at $t = 0$.The mathematical singularity is due to the use of Dirac delta function as the surface source. However, such a singularity and its neighborhood can be excluded from the elastic solutions for physical reality. Now, if $\bar{V}$ is negative, and the tangential stress is tensile at the outer surface and is greater than the critical value for crack generation, then fracture may occur near the outer surface in a short time. The principal shear stress $(\sigma_\theta - \sigma_r)/2$ near the outer surface decreases monotonically with increasing time for the case of instantaneous surface concentration source (See Fig. $2(c)$). Since the principal shear stress at the outer surface is very large at the initial time, plastic deformation may happen. The shear stress is always zero at the center.

The effect of the diffusivity ratio, D_A/D_B, on the principal stress components σ_r, σ_θ and the principal shear stress $(\sigma_\theta - \sigma_r)/2$ is shown in Figs. 3(a), (b) and (c), respectively for $\beta = 50$. At a given time, the magnitude of the radial stress at the center of layer A under the instantaneous surface source decreases monotonically with increasing δ/β or D_A/D_B (see Fig. $3(a)$). The magnitudes of tangential stress at both the outer surface and the center decrease with increasing δ/β. Also as δ/β (or D_A/D_B) increases, the tangential component becomes smaller and more uniformly distributed (Fig. 3(b)). As shown in Fig. 3(c), the principal shear stress $(\sigma_\theta - \sigma_r)/2$ decreases with increasing δ/β.

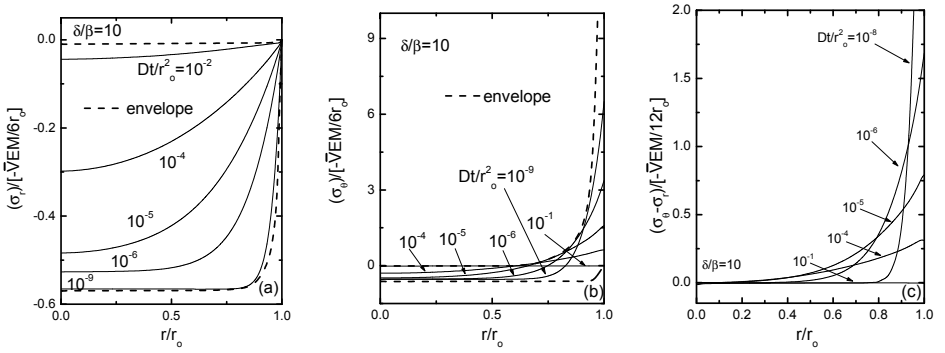

(a) (b) (c)

Figure 2: Stresses developed in layer A for different times at $\delta/\beta = 10$ under the instantaneous source diffusion: $(a)\sigma_r$, $(b)\sigma_\theta$ and $(c)(\sigma_\theta - \sigma_r)/2$. The curve termed envelope is composed of the extreme values of the stress at the given position during diffusion.

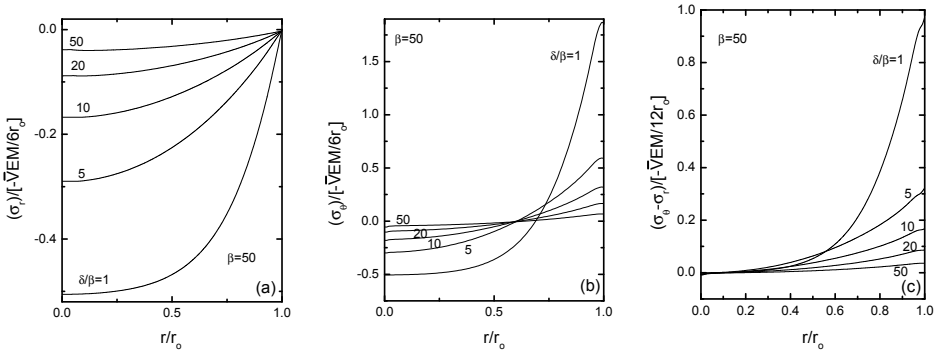

(a) (b) (c)

Figure 3: Stresses developed in layer A for different δ/β at $\beta = 50$ under the instantaneous source diffusion: $(a)\sigma_r$, $(b)\sigma_\theta$ and $(c)(\sigma_\theta - \sigma_r)/2$.

3.2 Constant surface concentration source

Substituting Eq. (9) into Eq. (14a) and Eq.(14b), we obtain the principal stresses for the constant surface concentration source. They are

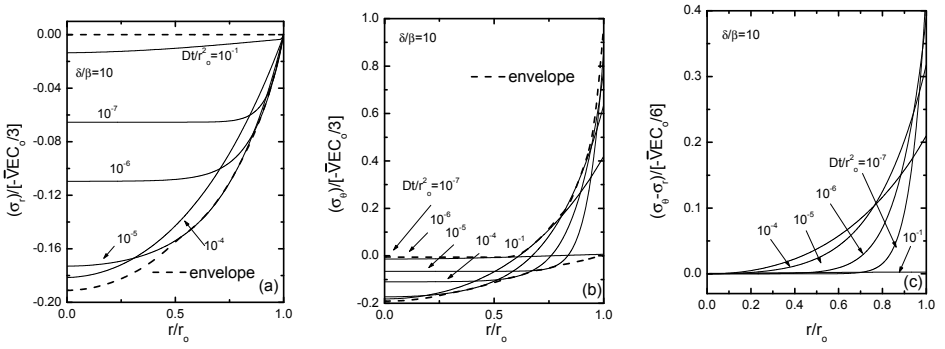

(a) (b) (c)

Figure 4: Stresses developed in layer A for different times at $\delta/\beta = 10$ under the constant source diffusion: $(a)\sigma_r$, $(b)\sigma_\theta$ and $(c)(\sigma_\theta - \sigma_r)/2$. The curve termed envelope is composed of the extreme values of the stress at the given position during diffusion.

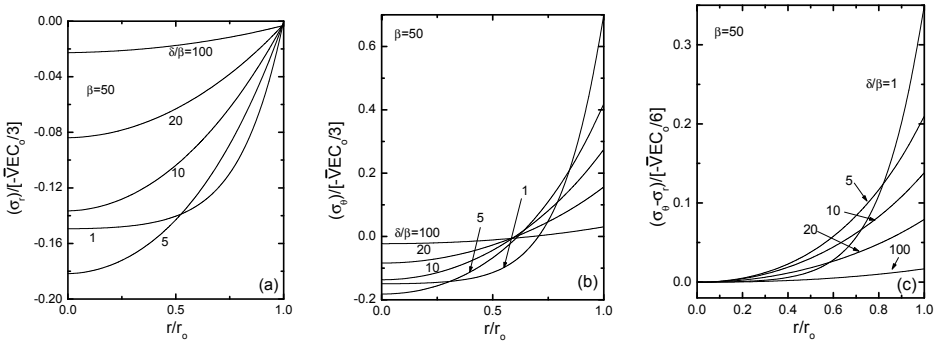

(a) (b) (c)

Figure 5: Stresses developed in layer A for different δ/β at $\beta = 50$ under the constant source diffusion: $(a)\sigma_r$, $(b)\sigma_\theta$ and $(c)(\sigma_\theta - \sigma_r)/2$.

$$\sigma_r = -\frac{2\overline{V}EC_0}{3}\sum_{n=1}^{\infty}\frac{1}{\alpha_n^2 J_1(\alpha_n)}\left[\frac{r_0}{r}J_1\left(\alpha_n\frac{r}{r_0}\right) - J_1(\alpha_n)\right] \times \exp\left[\left[\delta(\frac{\alpha_n}{\beta})^2\right]^2 - (\frac{\alpha_n}{\beta})^2\right] erfc[\delta(\frac{\alpha_n}{\beta})^2] \quad (17a)$$

$$\sigma_r = -\frac{2\bar{V}EC_0}{3}\sum_{n=1}^{\infty}\frac{1}{\alpha_n^2 J_1(\alpha_n)}\left[\alpha_n J_0\left(\alpha_n\frac{r}{r_0}\right) - \frac{r_0}{r}J_1(\alpha_n\frac{r}{r_0}) - J_1(\alpha_n)\right] \times \exp\left[[\delta(\frac{\alpha_n}{\beta})^2]^2 - (\frac{\alpha_n}{\beta})^2\right] erfc[\delta(\frac{\alpha_n}{\beta})^2] \quad (17b)$$

The stresses developed in the cylindrical sandwich composite under the constant surface concentration source are shown in Figs. 4(*a*)-(*c*) at $\delta/\beta = 10$. It is seen from Fig. 4(*a*) that at a given time, the radial stress is always maximum at the center r = 0 and is minimum and equal to zero at the outer surface $r = r_o$. The magnitude of the radial stress at the center increases to a maximum with increasing time and then decreases to zero. The evolution of radial stresses for this case, as shown in Fig. 4(a), is quite different from the case of the instantaneous concentration source (Fig. 2(a)). Note that the radial stress at the outer surface is always zero because the outer surface is traction-free. As shown in Fig. 4(*b*), the tangential stress at the outer surface and the center decreases with increasing time. It is found that the maximum tangential stress is equal to $-\bar{V}EC_0/3$ at $r = r_0$ and t = 0 (Note that $\sum_{n=1}^{\infty} 1/\alpha_n^2 = 0.25$.), and is greater than the maximum radial stress. If the partial molal volume is negative and the maximum tensile tangential stress is greater than the critical value for the generation of crack nucleus, the composite would fracture. The principal shear stress $(\sigma_\theta - \sigma_r)/2$ is shown in Fig. 4(*c*) at $\delta/\beta = 10$. Again the maximum value is located at $r = r_0$ and $t = 0$ with a magnitude of $-\bar{V}EC_0/6$. The other two principal shear stresses $(\sigma_r - \sigma_z)/2 = \sigma_r/2$ and $(\sigma_\theta - \sigma_z)/2 = \sigma_\theta/2$ can also be observed from Figs. 4(*a*) and 4(*b*), respectively. It can be seen from Fig. 4 that the two maximum principal shear stresses are equal to $-\bar{V}EC_0/6$ at $r = r_0$ and $t = 0$. If the maximum principal shear stress is greater than the critical value for dislocation generation, the sandwich composite would be plastically deformed.

The effect of diffusivity on the stresses developed in the sandwich composite at a constant surface concentration source is shown in Figs. 5(*a*)-(*c*) for $\beta = 50$. As shown in Fig. 5(*a*), the radial stress in the central region increases to a maximum with increasing δ/β and then decreases to zero. This trend is different from that under an instantaneous surface source, where the radial stress decreases monotonically with increasing δ/β (Fig. 3(*a*)). Since δ/β is equal to $a(D_A/D_B - 1)/r_o$ and a/r_o is constant, the effect of D_A/D_B on the radial stress at the center is most pronounced at a certain value of the ratio (more likely near δ/β=5 as shown in Fig. 5(a)). Fig. 5(*b*) illustrates that the tangential stress near the outer surface decreases monotonically with increasing δ/β, but the tangential stress in the central region has a similar trend as the radial stress. It can be seen from Fig. 5(c) that the principal shear stress $(\sigma_\theta - \sigma_r)/2$ near the outer surface decreases monotonically with increasing δ/β, similar to the case of instantaneous surface source (see Fig.3(c)).

Because D_A/D_B is coupled to a, the role of thickness a in the stress distributions is similar to that of the D_A/D_B. In summary, the tangential stress and the principal shear stress $(\sigma_\theta - \sigma_r)/2$ near the outer surface decreases with increasing D_A/D_B.

In addition to its local variation due to the concentration distribution, the chemical stress is also uniformly affected by the parameter $\overline{V}$, the partial molal volume. It is defined as the volume change, when one mole of solvent is replaced by an equal amount of sustitutional solute or is sharing the lattice with one mole of interstitial solute. Its value can be experimentally determined. In the case of wet oxidation of AlAs in the GaAs/AlAs/GaAs sandwich composite, the rate controlling process is the diffusion of H_2O in the reaction product Al_2O_3. The value of $\overline{V}$ for this system, however, has not been measured. For the purpose of illustration, an estimation of $\overline{V}$ is given below, based on the relation, $V = M/ N_A\rho$, where V is the volume of a single molecule (cm^3), M is the molecular weight (gm), N_A is the Avogadro's number, and ρ is the density (gm/cm^3). At room temperature, the density of H_2O is 0.997 gm/cm^3 and that of Al $_2O_3$is 3.95 gm/cm^3. The corresponding values of V are $18.1/N_A$ and $25.8/N_A$ cm^3. On the basis that the water molecule is substitutional, we obtain the value of $\overline{V}$to be –7.7 cm^3/mole. Such a volume decrement is likely to be a source of defect formation in the system.

4 Concluding Remarks

Since the chemical stress often causes the detrimental effect to a device, it would be very useful to have the information on its distribution and magnitude in the system. In this report, we present a detailed analysis of chemical stress induced by the boundary layer diffusion in a cylindrical sandwich composite of the BAB type. As usual, we considered two common diffusion processes, the constant surface source diffusion and the instantaneous surface source diffusion. The stress analysis was based on the linear elasticity.

The analysis shows that for a given time, all induced stresses, radial, tangential and the principal shear stresses, tend to be more uniformly distributed at a high diffusivity ratio in both diffusion processes. Also, at the source surface, both the tangential and the principal shear stresses decrease as the diffusivity ratio increases. In computing the stress distributions, some limiting values were determined. In the case of the constant surface source, the maximum tangential stress and the maximum principal shear stress are respectively $-\bar{V}EC_0/3$ and $-\bar{V}EC_0/6$, acting on the outer surface at the initial time. The corresponding maximum stresses in the case of the instantaneous source are infinite due to the use of Dirac delta function as the source concentration.

The general characteristics of the stress distributions induced in a cylindrical com-

posite during the boundary layer diffusion are similar to those in a rectangular composite. Irrespective of the geometry of the composites, the chemical stress increases as the diffusivity ratio, or the thickness of the central boundary layer, increases.

Acknowledgement: This work was supported by the National Science Council of Taiwan.

References

Bhandakkar, T.K.; Gao, H. (2011): Cohesive Modeling of Crack Nucleation in a Cylindrical Electrode under Axisymmetric Diffusion Induced Stresses. *Int. J. Solids Struct*. Vol. 48, pp. 2304-2309.

Christensen, J.; Newman, J. (2006): Stress Generation and Fracture in Lithium Insertion Materials. *J. Solid State Electrochem*. Vol. 10, pp. 293-319.

Choquette, K. D.; Geib, K. M.; Ashby, C. I. H.; Twesten, R. D.; Blum, O.; Hou, H. Q.; Follstaedt, D. M.; Hammons, B. E.; Mathes, D.; Hull, R. (1997): Advances in Selective Wet Oxidation of AlGaAs Alloys, *IEEE Selective Topics in Quantum Electronics,* Vol. 3, pp. 916-926.

Carslaw, H. S.; Jaeger, J. C. (1959): Conduction of Heat in Solids, Clarendon Press, Oxford, 2nd ed., Chap.12.

Crank, J. (1975): The Mathematics of Diffusion, Oxford University Press, London, 2nd ed., Chap. 5.

Deshpande, R.; Cheng, Y-T.; Verbrugge, M.W.; Timmons, A. (2011): Diffusion-Induced Stresses and Strain Energy in a Phase-Transforming Spherical Electrode Particle. *J. Electrochem. Soc.* 258, pp. A718-A724.

Deshpande, R.; Cheng, Y.-T.; Verbrugge, M.W. (2010): Modeling Diffusion–induced Stress in Nanowire Electrode Structures. *J. Power Sources* 195, pp. 2081-5088.

Dallesasse, J.M.; Holonyak, Jr., N.; Sugg, A.R.; Richard, T.A.; El-Zein, N. (1990): Hydrolyzation Oxidation of $Al_xGa_{1-x}As$-AlAs-GaAs Quantum Well Heterostructures and Superlattices. *Appl. Phys. Lett.* 57, pp. 394-396.

Deppe, G.D.; Huffaker, D.L.; Oh, T.H.; Deng, H.; Deng, Q. (1997): Low Threshold Vertical Cavity Surface-Emitting Lasers Based on Oxide-Confinement and High Contrast Distributed Bragg Reflector. *IEEE J. Sel. Topics Quantum Electron.* 3, pp. 893-904.

Guha, S.; Agahi, F.; Pezeshki, B.; Kash, J.A.; Kisker, D.W.; Bojarczuk, N.A. (1996): Microstructure of Al GaAs-oxide Heterolayers Formed by Wet Oxidation. *Appl. Phys. Lett.* 68, pp 906-908.

Huffaker, D.L.; Deppe, D.G.; Kumar, K.; Rogers, T.J. (1994): Native-Oxide Defined Ring Contact for Low Threshold Vertical-Cavity Lasers. *Appl. Phys. Lett.* 65, pp. 94-97.

Hayashi, Y.; Mukaihara, T.; Hatori, H.; OhnoKi, N.; Matsutani, A.; Koyama, F.; Iga, K. (1995): Record Low-threshold Index-guided InGaAs/GaAlAs Vertical-Cacity Surface-Emitting Laser with a Native Oxide Confinement Structure. *Electron. Lett.* 31, pp. 560-562.

Ko, S. C.; Lee, S.; Chou, Y. T. (2009): Radial Boundary Layer Diffusion in a Cylindrical Sandwich Composite with Application to Oxidation of GaAs/AlAs/GaAs, *Materials Chemistry and Physics*, 115, pp. 488-492.

Ko, S. C.; Lee, S.; Chou, Y. T. (2005): Chemical Stresses in a Square Composite, *Mater. Sci. Eng.*, A409, pp. 145-152.

Li, J. C. M. (1978): Physical Chemistry of Some Microstructural Phenomena. *Metall.Trans*, Vol.A9, pp. 1353-1380.

Lin, H.Y.; Ko, S. C.; Lee, S. (2004): Chemical Stresses in Boundary Layer Diffusion. *J. Appl. Phys.* 96, pp. 6183-6187.

Larson, M.C.; Coldren, C.W.; Spruytte, S.G.; Petersen, H.E.; Harris, J.S. (2000): Low-Threshold Oxide-Confined GaInNAs Long Wavelength Vertical Cavity Lasers. *IEEE Photon. Technol. Lett.* 12, pp. 1598-1600.

Miller, D. P.; Moore, J. E.; Morre, C. R. (1962): Boron Induced Dislocations in Silicon, *J. Appl. Phys.* 33, pp. 2648-2652.

Nishiyama, N.; Arai, M.; Shinada, S.; Suzuki, K.; Koyama, F.; Iga, K. (2000): Multi-Oxide Layer Structure for Single-Mode Operation in Vertical-Cavity Surface-Emitting Lasers. *IEEE Photon. Technol. Lett.* 12, pp. 606-608.

Prussin, S. (1961): Generation and Distribution of Dislocations by Solute Diffusion. *J. Appl. Phys*, Vol.32, pp. 1876-1881.

Read-Hill, R.E.; Abbaschian, R. (1994): Physical Metallurgy Principles. PWS Publishing Company, Boston, MA, 3^{rd} ed., Chapter 9.

Schwuttke,G.; H.Queisser, H. J. (1962): X-Ray Observations of Diffusion-Induced Dislocations in Silicon. *J. Appl. Phys*, Vol.33, pp. 1540-1542.

Timoshenko, S. P.; Goodier, J. N. (1970): Theory of Elasticity, McGraw Hill, London, 2^{nd} ed., Chap. 5.

Wang, W. L.; Chou, Y. T.; Lee, S. (1998): Chemical Stresses Induced by Grain Boundary Diffision," *Metall. Mater. Trans.* A29, pp. 2121-2125.

Wang, W. L.; Chou, Y. T.; Lee, S. (2001): Chemical Stresses Induced by Grain Boundary Diffusion in Thin Films, *J. Mater. Res.* 16, pp. 1967-1974.

Weigl, B.; Grabherr, M.; Michalzik, R.; Reiner, G.; Ebeling, K.J. (1996): High-Power Single-Mode Selectively Oxidized Vertical-Cavity Surface-Emitting Lasers. *IEEE Photon. Technol. Lett.* 8, pp. 971-973.

Whipple, R.T. (1954): Concentration Contours in Grain Boundary Diffusion. *Philos. Mag.* 45, pp. 1225-.1236.

Yang, F. (2010): Effect of Local Solid Reaching on Diffusion-induced Stress. *J. Appl. Phys.* 107, 103516.